

Supporting Information

H₂O₂ activated Ag₂S:In-Cu nanoprobe for in vitro synergistic tumor treatment

Xiaoyan Zhang^{1,#}, Ruiqi Liu^{2,#}, Zhouyu Yu¹, Baisong Chang^{*,1}

^a. State Key Laboratory of Advanced Technology for Materials Synthesis and Processing, Wuhan University of Technology, Wuhan 430070, China

^b. State Key Laboratory of Drug Research, Molecular Imaging Center, Shanghai Institute of Materia Medica, Chinese Academy of Sciences, Shanghai 201203, China

These authors contributed equally.

* Correspondence should be addressed to B.C. (chang@whut.edu.cn)

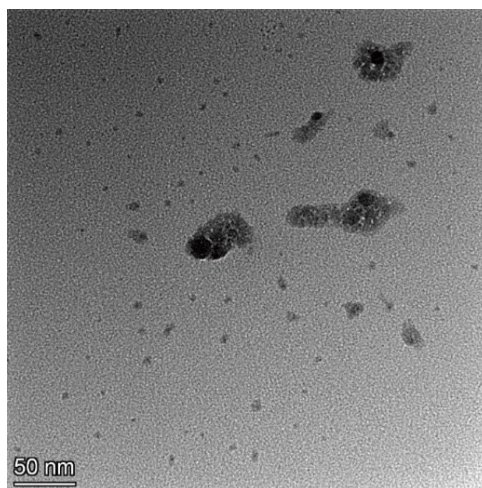


Fig. S1 TEM image of Ag_2S nanoparticles.

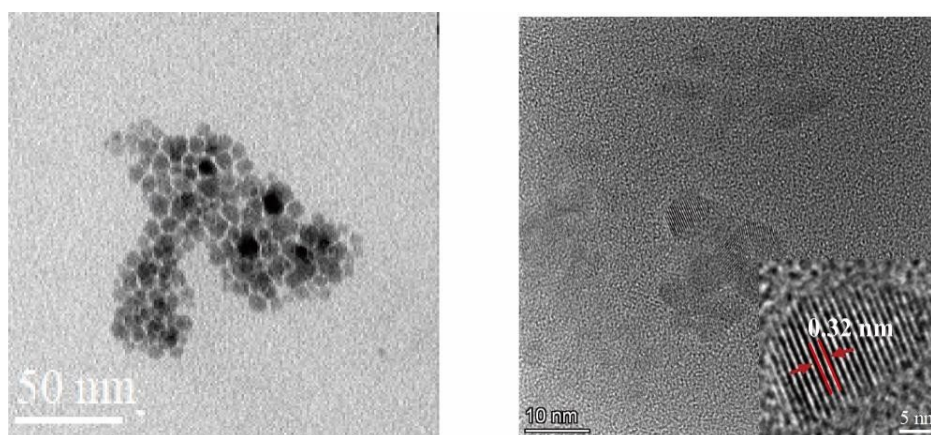


Fig. S2 TEM and high-resolution TEM images of AIS nanoparticles.

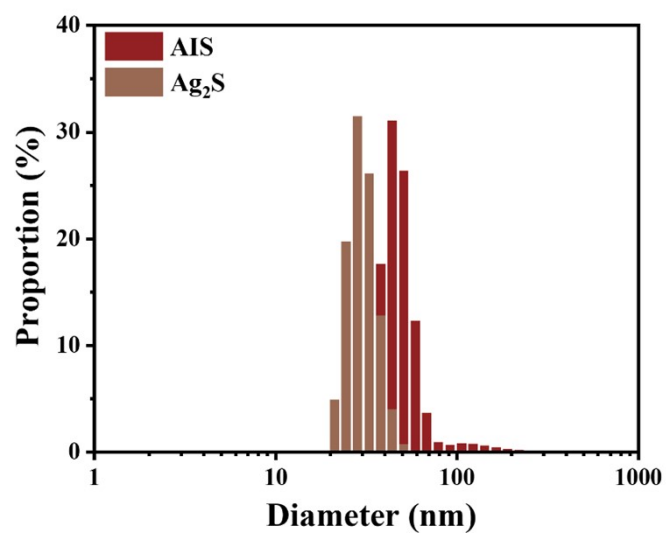


Fig. S3 Particle size of Ag_2S and AIS nanoparticles.

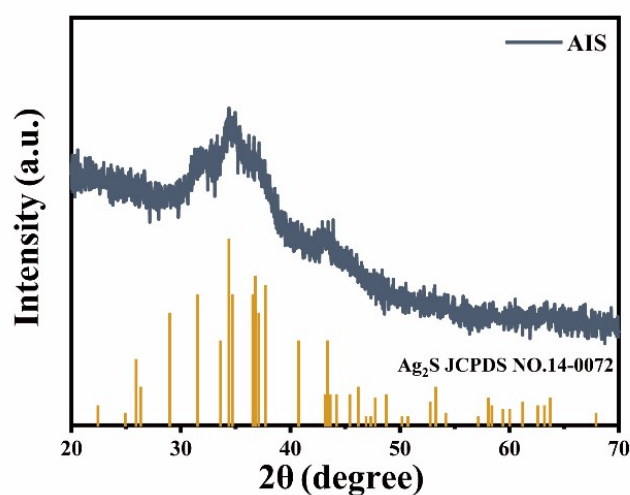


Fig. S4 X-ray diffraction pattern of AIS nanoparticles.

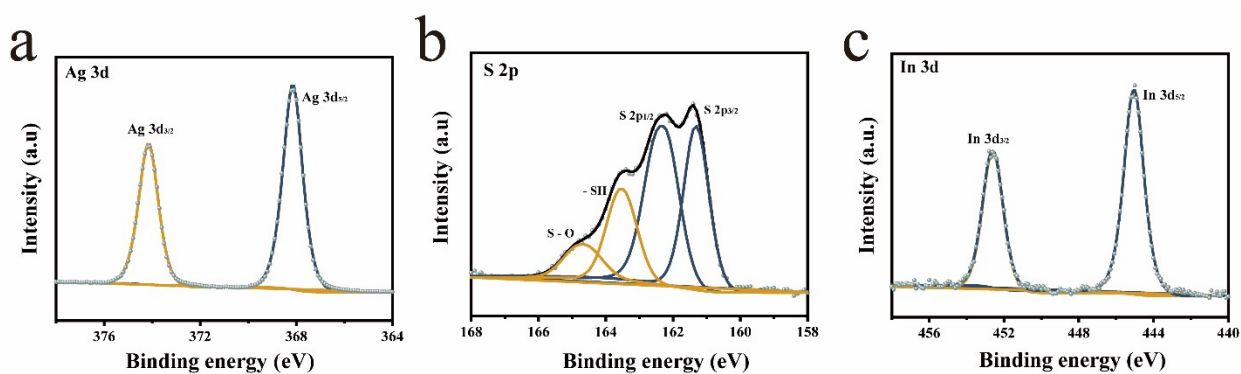


Fig. S5 Survey and fitted XPS analysis of AIS (Ag 3d, S 2p and In 3d) nanoparticles.

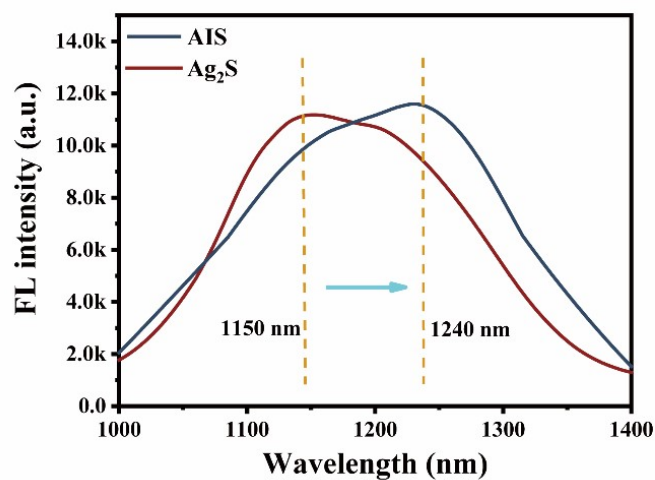


Fig. S6 NIR-II fluorescence spectra of AIS and Ag₂S nanoparticles.

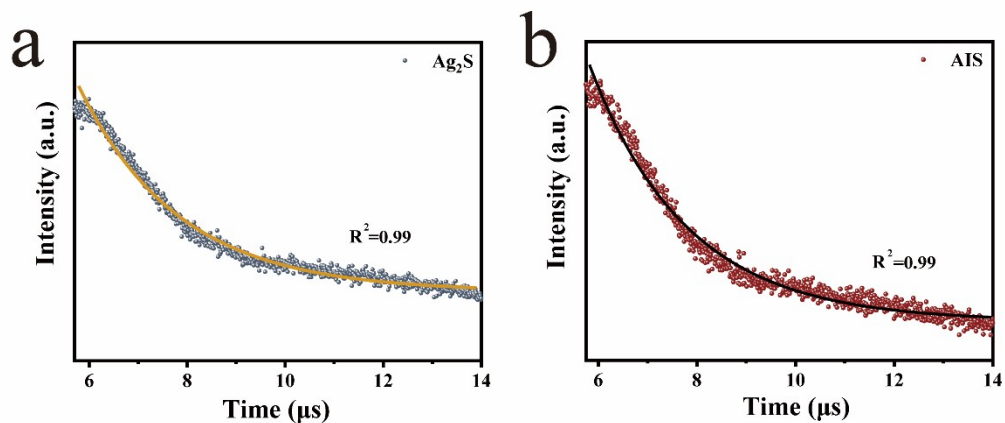


Fig. S7 Fluorescence lifetime of (a) Ag_2S and (b) AIS.

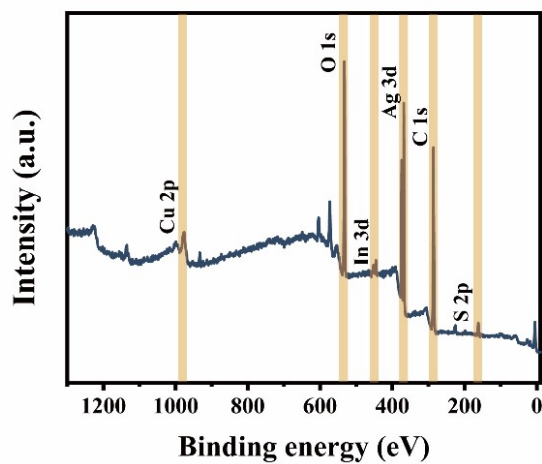


Fig. S8 XPS full spectrum of ACP nanoparticles.

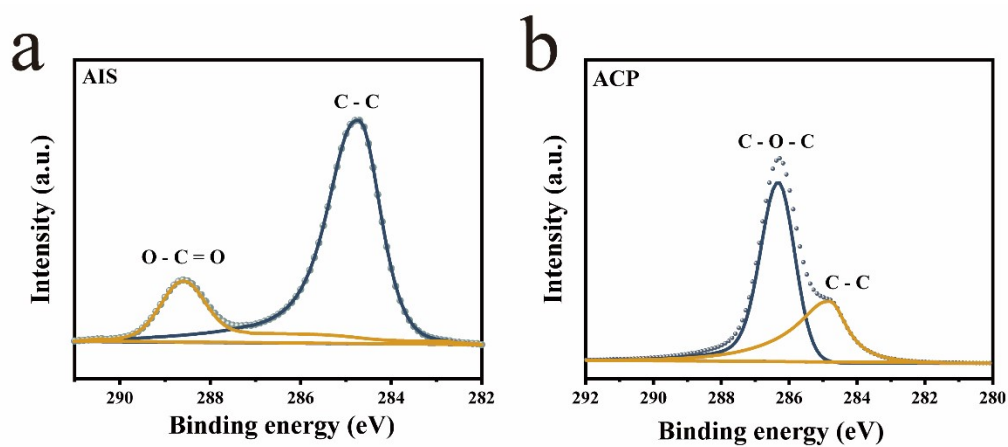


Fig. S9 High-resolution XPS spectra of C 1s. (a) AIS. (b) ACP.

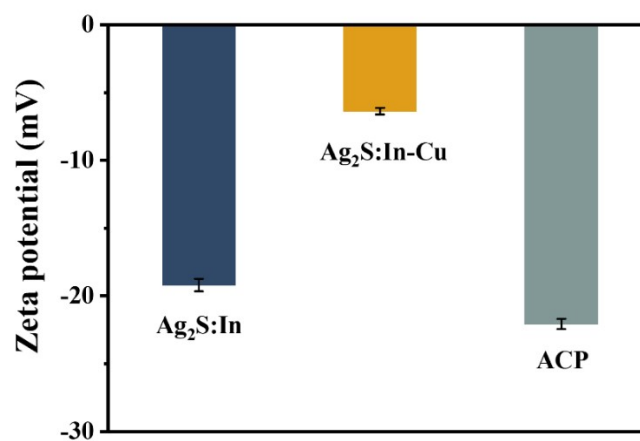


Fig. S10 Zeta potential measurement of Ag₂S:In, Ag₂S:In-Cu and ACP nanoparticles.

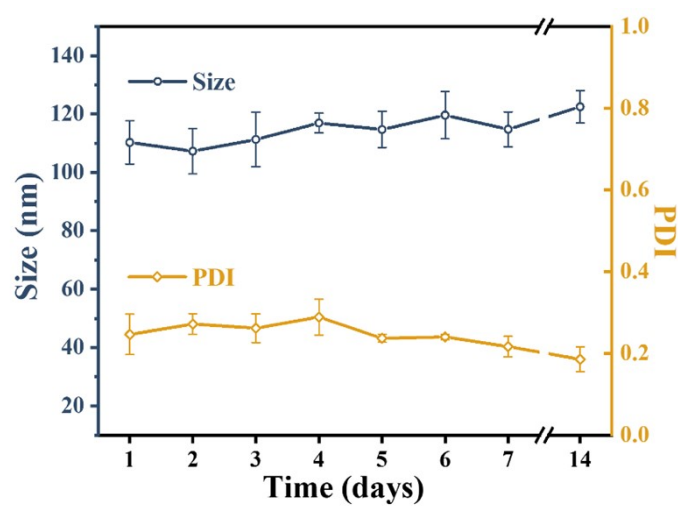


Fig. S11 Particle size and polymer dispersity index (PDI) during 14 days of ACP nanoparticles.

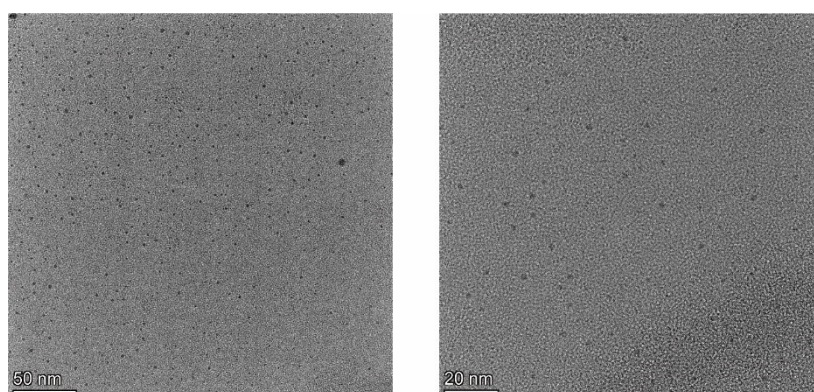


Fig. S12 TEM images of ACP nanoparticles treated with H₂O₂.

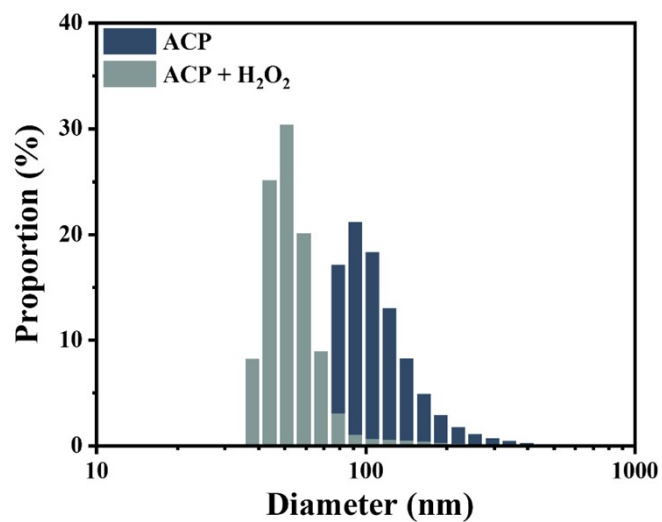


Fig. S13 Particle size of ACP and ACP treated with H₂O₂ nanoparticles.

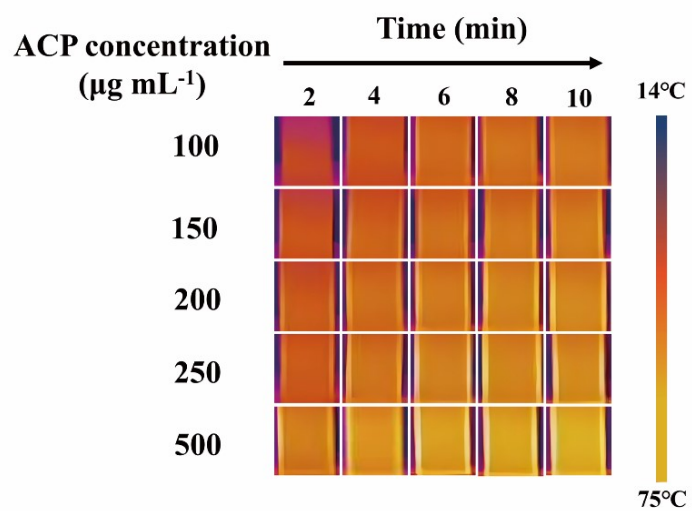


Fig. S14 Thermal images of ACP nanoparticles at different concentrations (0 - 500 µg mL⁻¹) under 808 nm laser irradiation for 10 min (2 W cm⁻²).

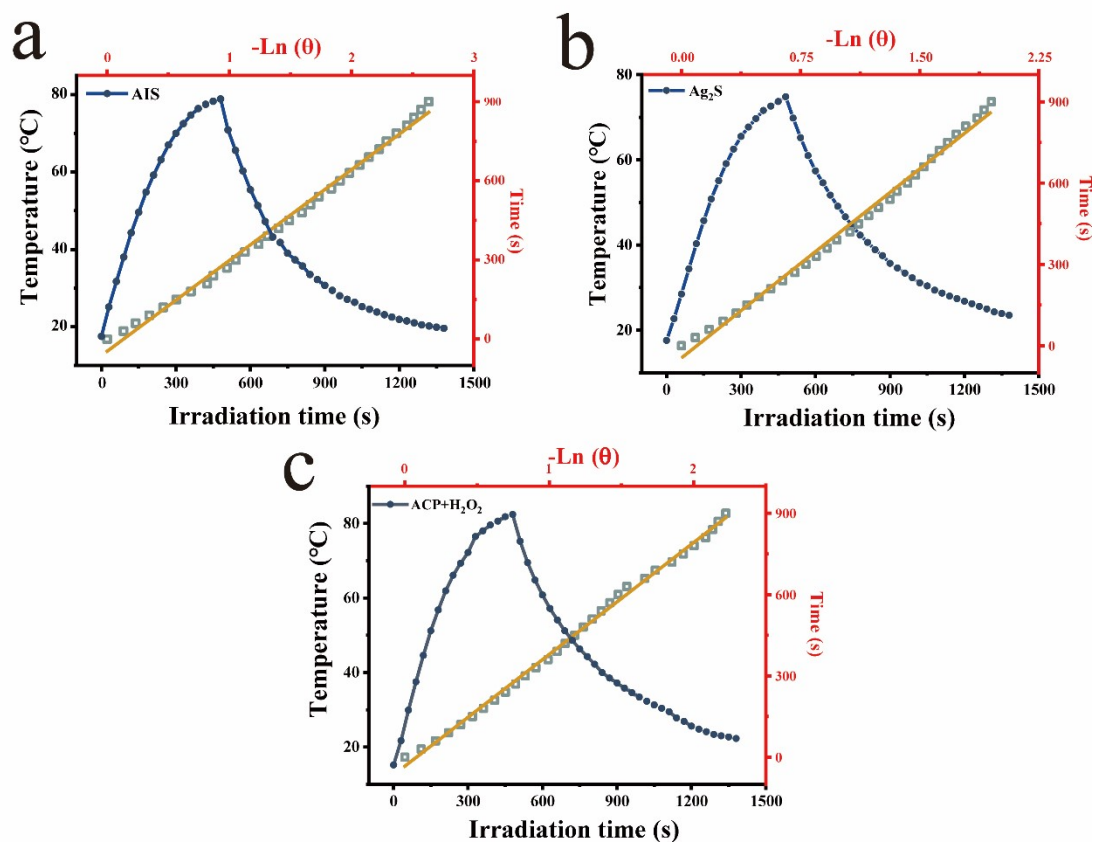


Fig. S15 (a, b, c) Temperature plots of the heating and cooling processes of AIS nanoparticles, Ag₂S nanoparticles and ACP nanoparticles treated with H₂O₂ irradiated with an 808 nm laser (2 W cm⁻²), and the plot of cooling time versus negative natural logarithm of the temperature driving force obtained from cooling stage.

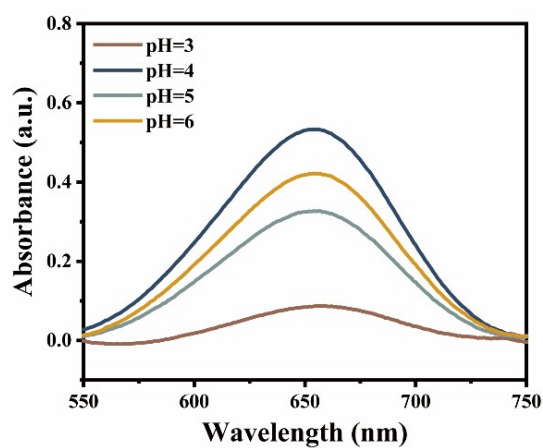


Fig. S16 The influence of different pH on ACP nanoparticles POD-like properties.

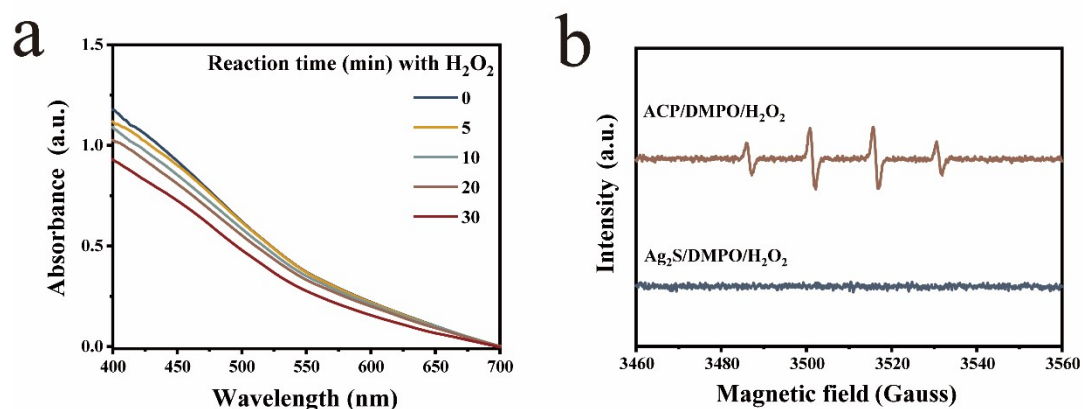


Fig. S17 (a) UV-vis spectra of Ag_2S nanoparticles and TMB/ H_2O_2 at different reaction times. (b) DMPO/ H_2O_2 treated with ACP nanoparticles and Ag_2S nanoparticles.

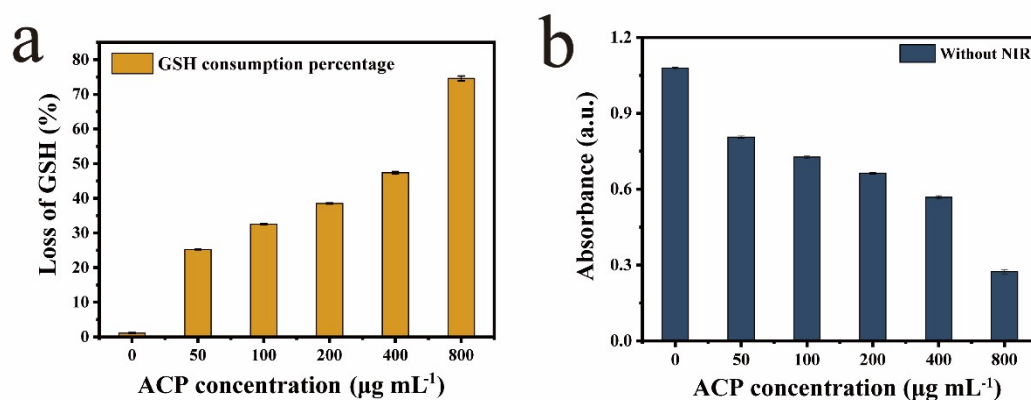


Fig. S18 (a) The percentage of GSH consumption and (b) absorbance change at 412 nm for different concentrations of ACP nanoparticles.

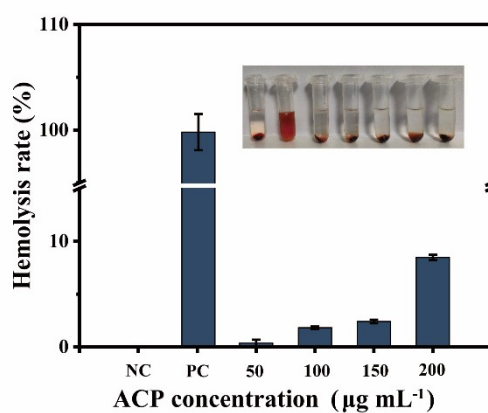


Fig. S19 Hemolysis rates of ACP nanoparticles with 3 h of incubation with blood cells (inset: hemolysis photo after centrifugation).

Table S1 PCE of some reported nanoparticles.

Nanoparticles	Power density (W cm ⁻²)	PEC (%)	Refs
PDA@Ag nanoparticles	1.0	36.1	[1]
SDBS-Ag ₂ Se nanoparticles	1.7	22.9	[2]
Ag ₂ S nanoparticles	1.0	38.5	[3]
Ag ₂ S/g-C ₃ N ₄ nanoparticles	2.5	31.3	[4]
BSA-Ag ₂ S nanoparticles	3.4	18.9	[5]
Ag ₂ S nanoparticles	2.0	41.0	[6]
ACP nanoparticles	2.0	54.0	This work

References

- [1] X. Qi, Y. Huang, S. You, Y. Xiang, E. Cai, R. Mao, W. Pan, X. Tong, W. Dong, F. Ye and J. Shen, *Adv. Sci.*, 2022, **9**, 2106015.
- [2] X. Yang, C. Wang, X. Zhang, Y. Wang, F. Gao, L. Sun, W. Xu, C. Qiao and G. Zhang, *Sci. Technol. Adv. Mater.*, 2020, **21**, 584-592.
- [3] S. Zhu, W. Song, Y. He, Y. Wang, X. Li, Y. Wu, X. Meng, C. Lin, W. Wang, H. Wang, S. Huang, F. Yan and L. Sun, *ACS Appl. Mater. Interfaces*, 2025, **17**, 37465-37478.
- [4] H. Wang, J. You, D. Shi, L. Cai, H. Shi and H. Shi, *ACS Appl. Nano Mater.*, 2024, **7**, 19904-19914.
- [5] J. Zhao, Q. Zhang, W. Liu, G. Shan and X. Wang, *Colloids Surf., B*, 2022, **211**, 112295.
- [6] R. Han, Y. Xiao, Q. Yang, M. Pan, Y. Hao, X. He, J. Peng and Z. Qian, *Biomaterials*, 2021, **264**, 120451.